15th IFK
Proc. of the 15th International Fluid Power Conference <Symposium/Conference>
<DOI>

Grain Microstructural Evolution of Friction Layers in Piston Pump Friction Pairs

Song Yuhan[1]* Angerhausen Julian[1] Schmitz Katharina[2]

[1] *Weichai Power European Science & Technology Innovation Center*

[2] *RWTH Aachen University – Institute for Fluid Power Drives and Systems (ifas)*

**Corresponding author: E-mail address: yuhan.song@weichaidestic.com*

Abstract.

In the frictional contact of piston pump friction pairs, the formation and evolution of the friction layer are accompanied by significant changes in the grain size, orientation, and distribution within the subsurface region. These grain-level structural characteristics critically influence the friction and wear behaviour of the contact interface. To clarify this process, cross-sectional EBSD (Electron Backscatter Diffraction) is carried out on specimens of port plate material after reciprocating sliding for different times under the same conditions. Changes in grain size, grain boundary misorientation angles, and crystal orientation reveal the rapid formation process of the friction layer. During the first hour of testing, the friction layer changes significantly. Grain size decreases, grain orientation rotation appears, and grain boundaries become pronounced with low-angle grain boundary (LAGB) to dominate. As the sliding continued, the layer thickness kept increasing until it stabilized after 2 h. From 2 h to 16 h, a stable hierarchical structure is established, consisting of an ultrafine-grained surface with persistent {111} alignment, an LAGB-rich transition zone, and the unaffected base material. These findings demonstrate that friction causes time-dependent stratification of microstructure and that the coupled evolution of refinement, boundary character, and orientation selection underpins the stability of the tribolayer, providing a quantitative basis for gradient design of wear-resistant hydraulic components.

Keywords. piston pump, friction layer, grain microstructure, EBSD.

1. INTRODUCTION

As a key element of hydraulic systems, axial piston pumps directly influence overall efficiency and reliability through their operational stability and durability. Under long-term high pressure and high-speed sliding, the friction surfaces gradually undergo wear , resulting in increased friction, lubrication deterioration, and leakage. This will reduce efficiency and durability, as well as cause damage to components. Therefore, an in-depth study of the wear mechanisms of key friction parts of piston pumps and their microstructural evolution is of great significance for extending service life and optimising lubrication design. Extensive research has been devoted to improving the tribological behaviour of piston pump components through surface texturing [1], operating-condition control [2], structural optimisation [3], material selection [4], coating design [5].

However, even with such optimisations, friction pairs inevitably experience a run-in stage. During this process, engineered systems transition from the initial state to a stable operating state by removing microscopic asperities via wear or plastic deformation, thereby improving surface conformity and friction stability [6]. R. Ivantysyn, et al analysed the running-in period of axial piston pumps, focusing on clarifying the effects of operating parameters and contact geometry on surface behaviour [7]. Tappeiner, et al. studied the optimisation of the surface roughness of the friction part of piston pumps, emphasising low friction and low wear achieved by matching the appropriate running-in mechanism with roughness parameters [8]. W. Jiao investigated the effects of initial surface roughness, speed and pressure on the tribological properties of axial piston pump port plate pairs under low-pressure conditions with respect to the run-in effect. The results show that higher speed and initial roughness shorten the run-in time, while higher pressure leads to an increase in the fluctuation amplitude of the friction coefficient. The wear mechanism is mainly characterised by abrasive wear [9]. A. Paulus studied the evolution of the friction layer when lead-free copper was used for the piston pair and found that under lubricated sliding contact conditions, both bronze and brass could form a stable boundary lubrication layer, and the formation mechanism was mainly attributed to the friction chemical reaction of tin oxide (SnO/SnO_2) and zinc sulphide (ZnS), which effectively reduced the coefficient of friction and improved the wear resistance [10]. At the contact interface, structural changes in the material can cover a depth range from a few nanometres (e.g., amorphization) to a few microns (e.g., phase transitions, recrystallization), which can lead to significant differences in the properties of the surface material compared to the substrate, including strength, corrosion resistance, lubrication properties, friction behaviour, and wear resistance [11].

Existing studies mainly focus on the macroscopic wear behaviour of the piston pump friction pair during the run-in stage, while there is a lack of systematic research on the microstructure evolution of the material during the run-in process and its influence on the tribological properties, as shown in Figure **1.1**. Especially, the evolution law of the microstructure of the piston pump friction pair still needs to be explored.

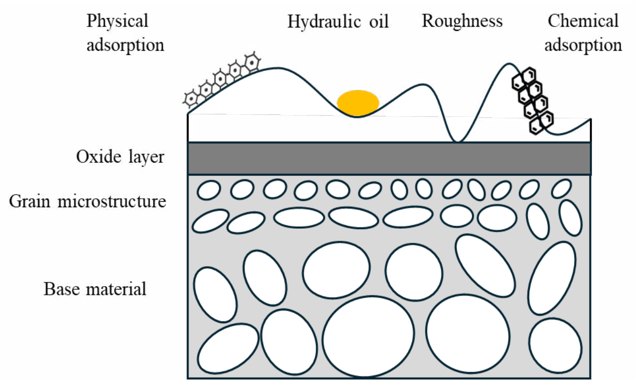

Figure 1.1. Schematic diagram of the microstructure of the friction layer

This study aims to systematically investigate the evolution of microstructure of the friction pairs from the running-in period to the steady state by using microanalysis techniques EBSD, and to analyse the characteristics of the friction layer's thickness, grain refinement, and orientation change in the process of friction, as well as their contribution to the wear resistance, to provide scientific basis for the optimization of the mating piston pump friction pair design.

2. MATERIAL AND METHODS

This section outlines the sample preparation, friction testing, and procedure for analysing the characterisation of friction layers.

2.1. Sample Preparation

Sample Preparation for friction test: the test specimens are the CuZn28Al4Ni3Si alloy, a widely used material for axial piston pump port plates due to its excellent wear resistance and mechanical properties. The specimens were machined into 24 mm × 6.9 mm discs, and surface roughness was controlled to Ra 0.4 µm, ensuring the same as the port plate surface. Before testing, all specimens were cleaned according to DIN 51834 standards, using ethanol and ultrasonic waves for cleaning, followed by drying with compressed air to remove residual contaminants. The other material in the friction pair consists of a QT600 steel pin with a diameter of 10 mm, which was manufactured and heat-treated in the same process as the cylinder block and installed as the upper test specimen.

2.2. Methods

The friction testing is performed on a sliding tribometer (SRV®5) in accordance with DIN 51834 standards. The test configuration consisted of a Pin-on-disc contact under lubricated conditions. The tribological experiments were conducted under the following conditions: frequency: 10 Hz、stroke length: 2 mm, normal load: 400 N, temperature: 50°C (preheating for 5 minutes before testing to ensure thermal stability), lubrication: mineral-based hydraulic oil (ISO VG 46 HLP46), refreshed before each test. Operating conditions remain constant, only time is varying. Six durations were set: 0.5 h, 1 h, 2 h, 4 h, 8, and 16 h, with three independent specimens per duration (N = 18).

To investigate microstructural evolution and crystallographic orientation, micrographs and orientation maps were obtained using a field-emission SEM (Zeiss Gemini SEM 500) equipped with an EBSD detector (Oxford Instruments Symmetry2). EBSD mapping was performed at an accelerating voltage of 20 kV, with a 120 μm aperture and a step size of 50 nm. After acquisition, the EBSD datasets were indexed and cleaned in Oxford Instruments, and subsequently processed to extract grain size statistics, grain boundary distributions, and grain orientation (inverse pole figure, IPF) by software.

Phase analysis was conducted using X-ray diffraction (XRD) with a Bruker D8 Advance diffractometer, equipped with a Cu-Kα radiation source (λ = 1.5406 Å). measurement conditions, scanning range: 5°–90° (2θ), step size: 0.02°, scan speed: 1°/min. The main purpose is to obtain an unknown phase of the material, which is passed to the EBSD test for phase determination.

2.3. EBSD Sample Preparation

Obtaining a complete subsurface grain-structure is challenging; sectioning and polishing must minimise the removal of tribolayer. Edge rounding caused by cutting, inlaying, or polishing can remove part of the tribolayer, cutting off the layer and making the actual thickness no longer measurable. To preserve the as-formed structure, cross-sections were prepared as follows: The wear-track surface was first sputter-coated with a thin Pt film to protect against local tearing during sectioning. At the centre of the friction zone, vertical to the sliding direction, a low-deformation cutting process is employed. To avoid edge rounding and prevent subsequent disassembly, specimens were inserted into hard conductive resin using a hot-dipping process, enabling direct analysis of the cross-section after insertion. The polishing process involved using SiC sandpaper (grit sizes ranging from 800 to 4000) until scratches were eliminated, followed by final chemical-mechanical polishing: colloidal silica (OPS, approximately 0.04 μm SiO_2) was applied at 50 rpm under low load (10 N) for 5 minutes to remove residual deformation layers. After polishing, the wear zone was re-inspected to confirm that the tribolayer remained continuous and was not polished, and the target region was marked with conductive adhesive. The specimen was then cleaned, dried, and examined by EBSD.

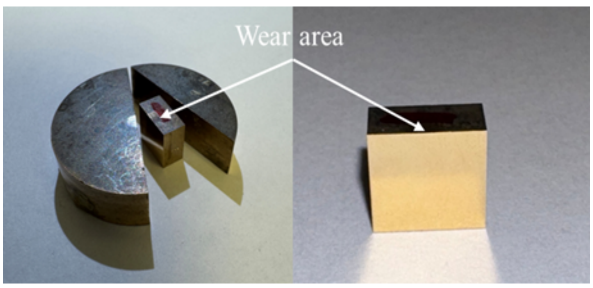

Figure 2.1. Sputter-Coated & Sectioned Specimen and Polished EBSD Cross-Section

3. RESULTS AND DISCUSSION

This section presents research findings spanning from tribological responses to subsurface mechanisms. Section 3.1 analyses friction-time behaviour, wear cross-sections, and the run-in and steady-state phases. Section 3.2, through X-ray diffraction combined with ICDD-PDF (International Centre for Diffraction Data – Powder Diffraction File) validation, analyses the phase composition of the distributor plate and provides critical background information for EBSD analysis. Section 3.3 employs EBSD techniques to investigate the depth-time distribution of equivalent grain size, grain boundary angle, and grain orientation across cross-sections at different time points.

3.1. Friction Behaviour and Surface Topography

In the study of hydraulic pump friction pairs, the coefficient of friction (COF) and wear are key parameters that characterise tribological performance. Both indicators are influenced by two concurrent mechanisms: material detaches from the surface, and on the other hand, the surface layer undergoes microstructural evolution under high stress and friction. These two mechanisms exist together under sliding lubrication conditions and directly influence the friction response and endurance of the friction pair.[12]

The evolution of the coefficient of friction over time is shown in Figure **3.1**. The results show the trend of the friction coefficient over time, presented as mean ± 1 standard deviation. The shaded areas indicate the standard deviation range with three specimens measured at each time point. During the initial 10 minutes (left figure), all groups showed low and quasi-constant friction coefficients. On a long-term scale (right figure, logarithmic time scale), the variability of the friction coefficient becomes more significant. The coefficient of friction increases between 0.5 h and 2 h. Between 2 h and 5 h, it remained at a high level with moderate fluctuations, before reducing again. Finally, after about 6 h, the coefficient of friction stabilized, with the range of the mean ± 1 standard deviation gradually narrowing, indicating that the system was approaching steady-state. This indicates that time dominates the evolution of friction behaviour. Regardless of the total test duration for individual specimens, results obtained at identical absolute time points remain consistent.

The curves for all specimens exhibit typical running-in characteristics: a rapid increase followed by a peak in the early stage, then a gradual decline toward stability. This closely aligns with Blau's summarised friction transition law, wherein the friction pair initially shows a rapid rise in the coefficient of friction before entering a stable wear phase [13].

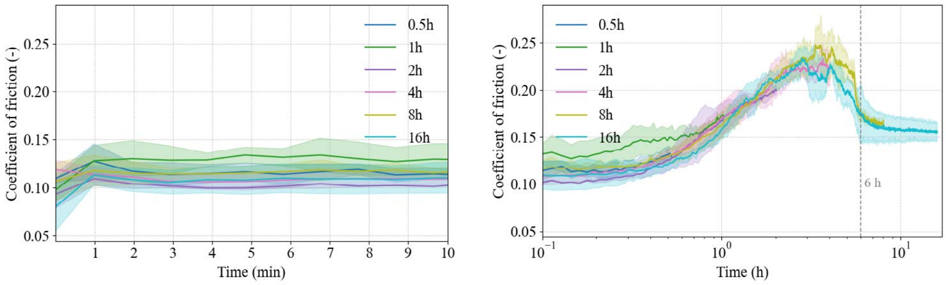

Figure 3.1. Time Evolution of the Coefficient of Friction

Within the first 6 h of measurement, the coefficient of friction changes significantly, indicating that the interface is still undergoing intense adjustment and the surface structure has not yet stabilised. As time progresses, the peak gradually decreases and its decay becomes more gradual, ultimately maintaining a low value and a stable range. This trend can be attributed to friction-induced grain refinement, changes in grain boundary angles and grain orientation [14–16]. The sustained friction process promotes the stabilisation of the surface microstructure, thereby effectively suppressing friction fluctuations.

The cross-sectional profiles of the wear scars (Figure **3.2**) illustrate the temporal evolution of wear depth. At the early stage (0.5 h and 1 h), the wear scars are shallow, and the cross-sections appear relatively smooth, indicating that the material removal is primarily governed by surface plastic deformation accompanied by slight delamination. By 2 h and 4 h, the wear depth increases significantly, and the cross-sections evolve into sharp “V-shaped” grooves. When the sliding time is further extended to 8 h and 16 h, the wear depth reaches its maximum. The good correlation between wear depth and friction coefficient indicates that the system is transitioning from run-in phase to steady-state friction.

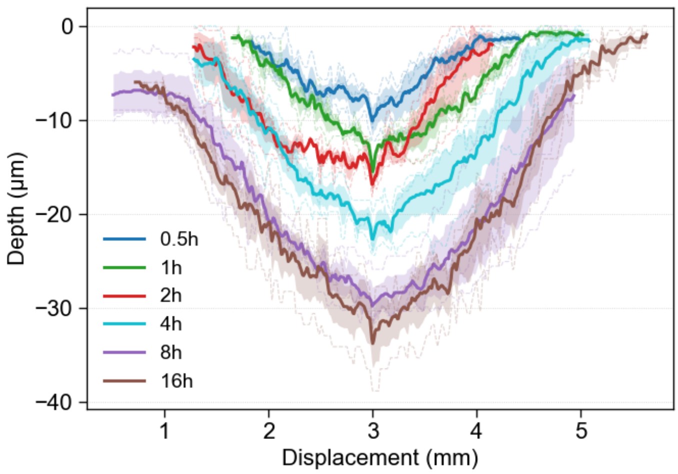

Figure 3.2. Central Groove Profile vs. Time

From a contact mechanics perspective, in the early stages of contact, the interaction is point-to-surface, resulting in extremely high localised stresses that easily lead to strong plastic deformation and ploughing, which increases the friction coefficient. As sliding progresses, the actual contact area increases and becomes more conforming, with the point-to-surface contact gradually transitioning to surface-to-surface contact. The bottom of the wear scar changes from flat to curved, and the contact state tends toward stability [17–19].

However, the above observations primarily reflected friction responses, revealing limited insights into the of the friction layer mechanisms. To uncover this, cross-sectional EBSD was used to construct depth–time maps, tracking grain refinement, orientation selection, and boundary evolution and relating these to friction and wear. This microstructure-to-property linkage clarifies how the tribolayer forms, evolves, and reaches a steady state.

3.2. Phase Identification

The XRD pattern of the port plate material is shown in Figure **3.3**. It displays the XRD diffraction pattern of the end plate material, analysed in conjunction with reference PDF cards for potential constituent phases. The diffraction peaks correspond to three phases: Co_3Ni, CuZn, and $Cu_{0.66}Zn_{0.34}$. Among these, only a faint Co_3Ni diffraction peak was detected, indicating an extremely low content of this phase.

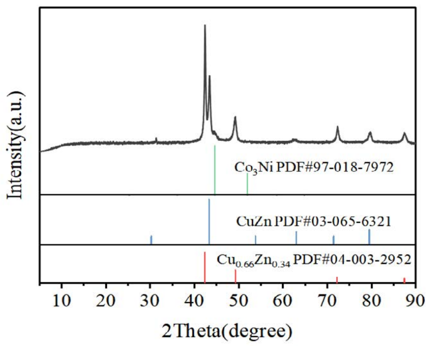

Figure 3.3. The XRD pattern of the port plate material

The results show that this phase belongs to the FM3M space group and has a face-centred cubic (FCC) structure. By analysing the diffraction peaks, the crystal structures of each phase were determined, providing fundamental data for the following EBSD testing. This can help deeply understand the microstructural characteristics of the port plate and their impact on material properties.

3.3. Time-dependent evolution of the microstructure of the friction layer

Figure **3.4** shows the SEM cross-section at 8 h: the interface is generally smooth, with no through-peeling observed, nor significant edge rounding, chamfering, or polishing marks, indicating that the sample preparation process preserved the true form of the friction layer.

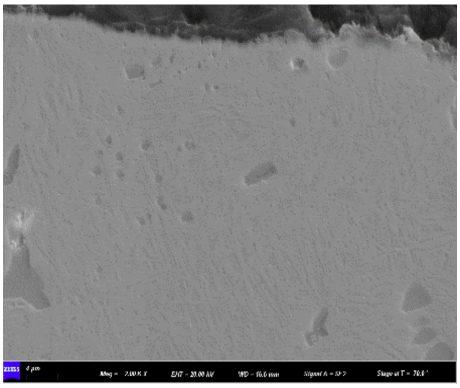

Figure 3.4. Cross-Sectional SEM at 8 h (Wear-Track Centre)

Figure **3.5** shows the EBSD results, with three results for each time point, only one of them is displayed here. All maps are displayed as IPF-ND (normal direction) colourings, with orientations defined by the accompanying inverse pole-figure triangle (red is {001}, green is {110}, blue is {111}). High-angle grain boundaries (HAGB, ⩾15°) are shown in black line; low-angle grain boundaries (LAGB, 2–15°) in green line. Regions affected by severe plastic deformation or delamination, as well as exogenous large particles (third-body debris), were masked and excluded from quantitative statistics. Near-surface nanograins approach the EBSD step-size and pattern-quality limits; values in this range should be regarded as lower-bound estimates.

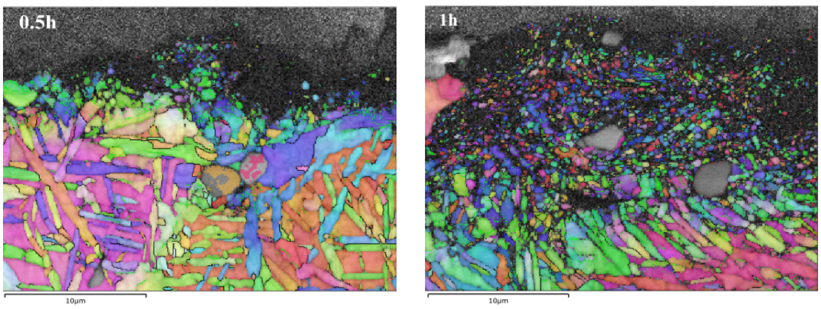

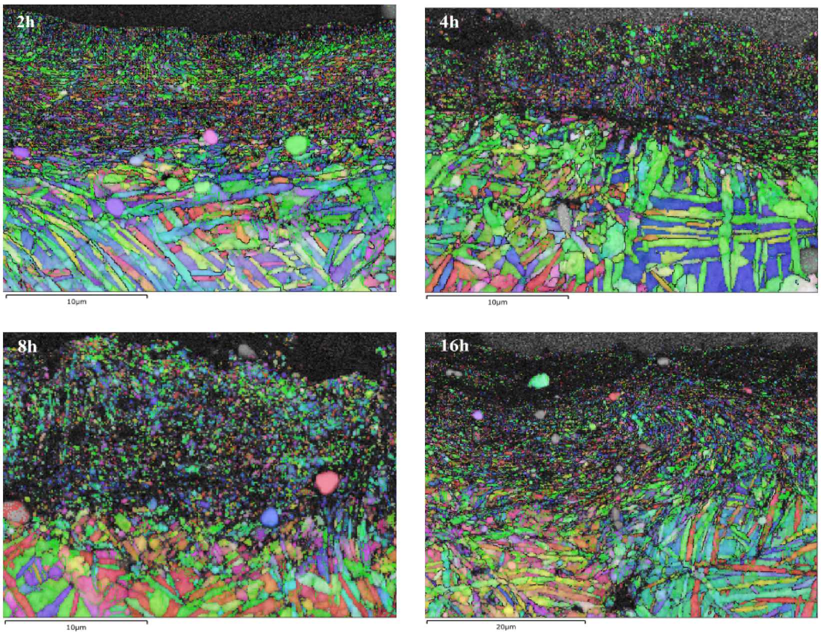

Figure 3.5. Time evolution of the friction layer cross-section at the centre of the grinding mark (0.5 h–16 h)

Grain Size Analysis. EBSD results show that the friction layer at different friction times shows a significant delamination and refinement: surface grains are clearly refined, while base material grains remain large and almost unaffected [20]. At 0.5 h, the friction layer was thinnest, with surface grains appearing refined, indicates that in the early stage, the local high stress and friction were already enough to cause a significant plastic deformation [21]. By 1 h, the fine-grain layer had significantly thickened and expanded, though its grain size remained larger than that at 2 h. Concurrently, EBSD images revealed external grains from the counter-friction material embedded within the copper alloy friction layer, indicative of third-body inclusion during friction [22]. At 2 h, the layer rapidly increases in thickness and reaches a local peak, indicating the intense surface refinement and rapid evolution during the early friction stage. From 2 h to 16 h, the friction layer thickness no longer increased significantly but stabilized at a higher thickness., as shown in Figure **3.6**. The layer thickness is defined as the combined thickness of the ultrafine-grained surface layer and the transition layer, excluding the unaffected base material. The gray dots represent individual sample measurements, while the gray shaded areas denote the mean ± 1 standard deviation for all samples at each time point, the black line as a trend reference.

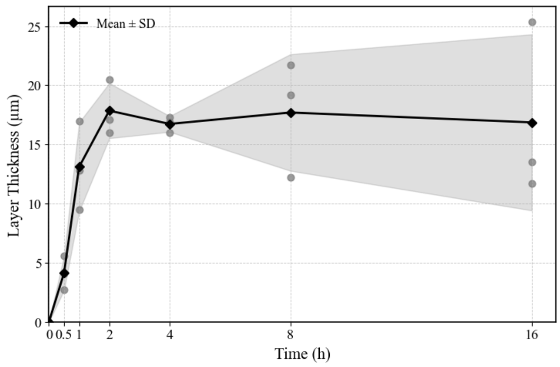

Figure 3.6. Thickness of the Friction-Induced Layer vs. Time

With increasing depth, the grain size increases gradually, with a medium-grain transition layer in the middle and the substrate grains forming the bottom layer. This gradient indicates that friction energy dissipates primarily at the surface and subsurface regions, decreasing with depth [23]. This evolution stems from the competition between grain refinement and surface spalling: on one hand, continuous friction and energy input promote the formation of new fine grains, while on the other, repeated sliding induces localized exfoliation and material removal [24,25].The early rise in COF matches the wear phase dominated by spalling; its decrease and subsequent stabilization match the phase where friction layer refinement/regeneration prevails. As the layer structure stabilizes, COF converges towards a steady state.

Grain Boundary Angle Analysis. Figure **3.7** shows the proportion of LAGB at different time points. At 0.5 h, low-angle grain boundaries appear in the outermost layer. At this stage, grains exhibit slight refinement accompanied by a large number of low-angle grain boundaries. The proportion of surface LAGB significantly increased, far exceeding that of the base phase. However, by 2 h, a distinct further stratification becomes evident: the surface layer consists of fine grains and a small proportion of high-angle grains (27.6%); the subsurface layer contained larger grains than the surface layer but exhibited a high proportion of low-angle grain boundaries (68.4%); the deepest layer comprised the base material (26.8%). During the long-term stage (8 h–16 h), as shown in Figure 3.5, the surface layer kept a low proportion of LAGB, while the subsurface layer maintained a significant proportion.

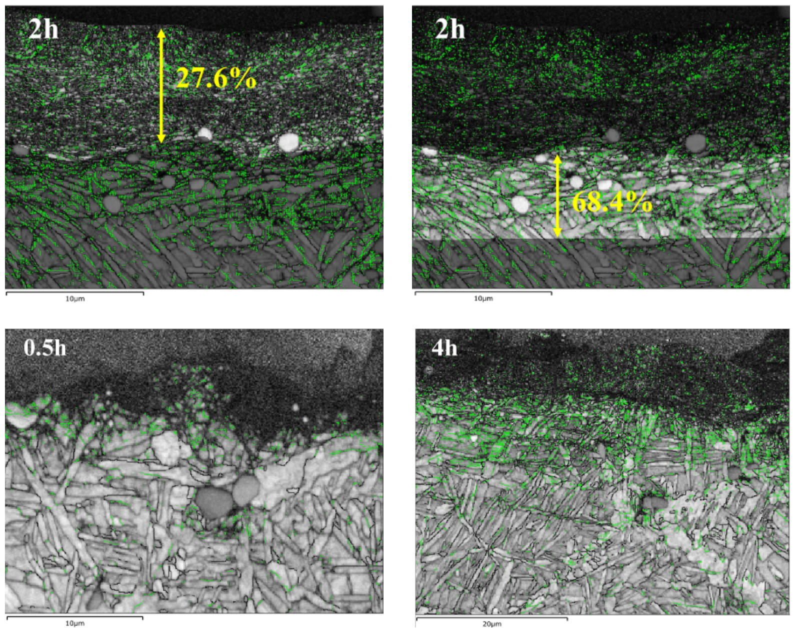

Figure 3.7. Distribution of Low-Angle Grain Boundaries

This indicates that during friction, grains first undergo dislocation or slip, leading to an increase in low-angle grain boundaries and the initiation of grain refinement. As friction persists and energy is continuously input, grain size further refines, and low-angle grain boundaries begin to transform into high-angle grain boundaries.

Before 2 h, the transition zone within the friction layer was not clearly defined. At this stage, the proportion of small-angle grain boundaries in the surface layer initially increased and then decreased. After 2 h, a distinct transition region emerged within the friction layer: grains of moderate size containing a significant number of small-angle grain boundaries. The surface layer and its evolution over time are shown in Figure **3.8**.

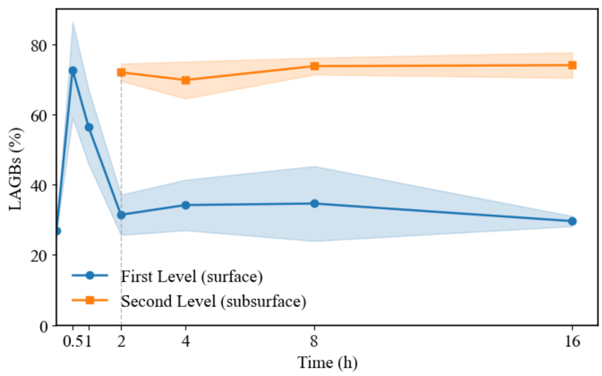

Figure 3.8. Time Evolution of Grain-Boundary Distribution in the Tribolayer

The friction process progressively establishes and maintains a stable delamination structure: fine-grained layers with a high proportion of HAGB surface layers, a large number of LAGB transition zones, and base grain boundaries.

The formation of this stratified structure can be attributed to two mechanisms. First, part of the LAGB in the surface layer gradually undergoes orientation rotation under continuous shear and evolves into HAGB, leading to structural stabilisation. Second, the surface experiences cyclic delamination while former subsurface layer transforms to surface layer. Strain is primarily accommodated in the subsurface, thereby maintaining a high fraction of LAGB in that region [26]. The evolution of microstructure is primarily confined to the friction layer and transition area, with the deeper base material remaining largely unaffected by this process and keeping its original grain boundary characteristics.

Grain Orientation Analysis. To quantify the temporal evolution of crystallographic orientation, the surface normal direction (ND) was taken as the reference for EBSD-based IPF analysis. In the base material, due to the properties inherent to casting and processing conditions, grain orientation remains essentially random. After sliding, however, the surface layer of most specimens consistently exhibits a pronounced {111} texture, while the subsurface retains a more random orientation distribution. This trend is evident in both short-term (0.5 h) and long-term (16 h) specimens, as shown in Figure **3.9**.

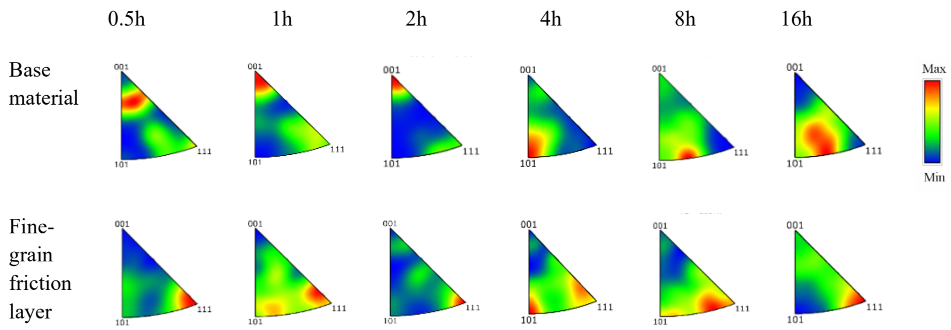

Figure 3.9. Time-Dependent Evolution of Grain Orientation

The evolution of grain orientation toward {111} can be explained by two mechanisms. First, during repeated sliding, surface grains are subjected simultaneously to tangential shear stress and normal contact stress, which induce progressive grain rotation. The rotation path is mainly governed by the sliding direction (SD), transverse direction (TD), and the initial orientation of each grain [16,27]. For FCC copper alloys, the combined shear and normal stresses during friction drive grains to rotate until their orientations align with the most easily activated and mechanically stable slip system. In this case, the favourable orientation is {111}, resulting in the predominance of {111}-oriented grains at the surface. The second mechanism is orientation selection: grains with less wear-resistant orientations are more prone to removal during sliding, leaving behind grains with the more stable and wear-resistant {111} orientation.

4. CONCLUSIONS

1) Under boundary lubrication, a friction layer forms on the planar distributor plate within around 0.5 h; surface grains are rapidly refined, with a significant {111} orientation and a higher proportion of LAGB grains.
2) The thickness of the tribological layer increases over time; after 2 hours, it shows a fluctuation pattern with a cycle of "formation-detachment-reformation," and the peak thickness no longer increases monotonically.
3) After 2 h, the LAGB proportion decreases and the friction layer enters a stable delamination state: the surface layer consists of ultrafine grains of {111} with less LAGB; the subsurface layer beneath is oriented and dispersed, enriched with LAGB, and has slightly larger grains; the base layer extends further downward.
4) The friction layer stabilisation and friction coefficient decrease occur concurrently, showing that grain-scale micro-evolution directly influences macro-scale tribological properties.

5. SUMMARY AND OUTLOOK

5.1. Summary

This study demonstrates that the friction layer of the distributor undergoes systematic evolution with increasing friction duration. Within a short timeframe, surface grain refinement occurs, LAGB increases, and preferred orientation develops. As friction time increases, ultrafine grains form in the surface layer, exhibiting preferred orientation and an increased proportion of HAGB; the subsurface layer contains numerous LAGB with larger grain sizes than the surface layer and random grain orientation. The stable emergence of this friction layer coincides with the oscillatory decrease in the coefficient of friction, indicating that the evolution of the friction layer governs the friction and wear of the distributor plate. This provides a basis for designing wear-resistant port plates.

5.2. Outlook

Although this study has clarified the time series evolution and formation mechanism of the friction layer, two questions still require answers. The specific effects of variable load pressures and shear stresses on grain-level microstructural evolution, along with their direct correlation to wear resistance, have not been quantitatively established. Furthermore, the structural evolution processes at finer scales before observable changes in grain size and orientation require further clarification. On this basis, effective stabilisation mechanisms for the friction-induced layer can be developed, providing a route to significantly enhance the wear resistance and operating efficiency of hydraulic pump friction pairs.

6. REFERENCES

[1] X. Ma, Q.J. Wang, X. Lu, V.S. Mehta, 'Piston surface design to improve the lubrication performance of a swash plate pump', Tribology International, pp. 275–285, Apr., 2019.

[2] M. Ivantysynova, R. Lasaar, 'An Investigation into Micro- and Macrogeometric Design of Piston/Cylinder Assembly of Swash Plate Machines', International Journal of Fluid Power, pp. 23–36, Jan., 2004.
[3] G. Schuhler, A. Jourani, S. Bouvier, J.-M. Perrochat, 'Wear mechanisms in contacts involving slippers in axial piston pumps: A multi-technical analysis', Journal of Materials Engineering and Performance, pp. 5395–5405, Oct., 2018.
[4] H. Wu, L. Zhao, S. Ni, Y. He, 'Study on friction performance and mechanism of slipper pair under different paired materials in high-pressure axial piston pump', Friction, pp. 957–969, Oct., 2020.
[5] A. Holzer, S. Koss, J. Rosefort, J.H. Schleifenbaum, K. Schmitz, 'EHLA-Coated Carbide-Reinforced Control Plates in Axial Piston Pumps First Results from Real-Life Application', Advances in Hydraulic and Pneumatic Drives and Control 2023, pp. 238–248, 2024.
[6] J. Jamari, 'Running-in as an engineering optimization', J@ Ti Undip: Jurnal Teknik Industri, pp. 1–10, 2007.
[7] R. Ivantysyn, A. Shorbagy, J. Weber, 'Analysis of the run-in behavior of axial piston pumps', 2018 Global Fluid Power Society PhD Symposium (GFPS), pp. 1–9, Samara, Jul., 2018.
[8] Z. Tappeiner, A. Holzer, K. Schmitz, 'Experimental development and validation of tribological run-in strategies to reduce friction in hydraulic applications', Tribologie und Schmierungstechnik, May, 2024.
[9] W. Jiao, Y. Xia, H. Ma, Z. Zhu, S. Xia, 'Effect of running-in on the low-pressure tribological performance of valve plate pair in axial piston pumps', Wear, p. 205113, Nov., 2023.
[10] A. Paulus, 'Reaktionsschichtbildung auf bleifreien bronze- und messingwerkstoffen im kontakt von zylinder und steuerscheibe einer axialkolbenpumpe', Doctoral Dissertation, RWTH Aachen University, Aachen, 2017.
[11] H. Czichos, K.-H. Habig, 'Tribologie-handbuch: tribometrie, tribomaterialien, tribotechnik', Springer-Verlag, 2010, ISBN: 3-8348-9660-8.
[12] A. Kapoor, J.A. Williams, K.L. Johnson, 'The steady state sliding of rough surfaces', Wear, pp. 81–92, 1994.
[13] P.J. Blau, 'On the nature of running-in', Tribology International, pp. 1007–1012, Nov., 2005.
[14] D.A. Rigney, 'Large strains associated with sliding contact of metals', Materials Research Innovations, pp. 231–234, Mar., 1998.
[15] H.A. Padilla, B.L. Boyce, C.C. Battaile, S.V. Prasad, 'Frictional performance and near-surface evolution of nanocrystalline ni–fe as governed by contact stress and sliding velocity', Wear, pp. 860–871, Jan., 2013.
[16] C. Haug, D. Molodov, P. Gumbsch, C. Greiner, 'Tribologically induced crystal rotation kinematics revealed by electron backscatter diffraction', Acta Materialia, p. 117566, Feb., 2022.
[17] S. Becker, K. Schulz, D. Scherhaufer, P. Gumbsch, C. Greiner, 'Variations in strain affect friction and microstructure evolution in copper under a reciprocating tribological load', Journal of Materials Research, pp. 970–981, Feb., 2021.
[18] J.R. Barber, 'Contact mechanics', Vol. 20, Springer, 2018, ISBN: 978-3-319-70938-3.

[19] X. Chen, Z. Han, K. Lu, 'Friction and Wear Reduction in Copper with a Gradient Nano-grained Surface Layer', ACS Applied Materials & Interfaces, pp. 13829–13838, Apr., 2018.
[20] C. Greiner, Z. Liu, L. Strassberger, P. Gumbsch, 'Sequence of Stages in the Microstructure Evolution in Copper under Mild Reciprocating Tribological Loading', ACS Applied Materials & Interfaces, pp. 15809–15819, Jun., 2016.
[21] F. Ruebeling, Y. Xu, G. Richter, D. Dini, P. Gumbsch, C. Greiner, 'Normal load and counter body size influence the initiation of microstructural discontinuities in copper during sliding', ACS Applied Materials & Interfaces, pp. 4750–4760, Jan., 2021.
[22] K.C. Ludema, 'Third bodies: perspectives on modeling in lubricated contacts, in close fitting contacts, etc: following on the concepts of dr. Maurice godet', pp. 3–19, Jan., 1996.
[23] M. Chandross, N. Argibay, 'Friction of metals: A review of microstructural evolution and nanoscale phenomena in shearing contacts', Tribology Letters, p. 119, Dec., 2021.
[24] N. P. Suh, 'The delamination theory of wear', Wear, pp. 111–124, Jul., 1973.
[25] M.M. Khonsari, S. Ghatrehsamani, S. Akbarzadeh, 'On the running-in nature of metallic tribo-components: A review', Wear, p. 203871, Jun., 2021.
[26] D.A. Hughes, N. Hansen, 'High angle boundaries formed by grain subdivision mechanisms', Acta Materialia, pp. 3871–3886, Sep., 1997.
[27] C. Haug, F. Ruebeling, A. Kashiwar, P. Gumbsch, C. Kübel, C. Greiner, 'Early deformation mechanisms in the shear affected region underneath a copper sliding contact', Nature Communications, p. 839, Feb., 2020.

Biographies

Yuhan Song received bachelor's degree in Mechanical Design, Manufacturing and Automation from Taiyuan University of Science and Technology in 2015, the master's degree in Engineering Mechanics from Taiyuan University of Science and Technology in 2018. His professional experience includes serving as a Hydraulic Component Development Engineer at Linde Hydraulic China (August 2018-June 2021), a Component Simulation Engineer at Linde Hydraulic Germany (July 2021-June 2023), and currently as a Hydraulic Component Development Engineer at Weichai Power European Science & Technology Innovation Center (July 2023-present). His primary research focus encompasses the development and simulation of hydraulic components, including pumps, motors, and valves.

Dr. Julian Angerhausen received his bachelor's degree (2012), master's degree (2014), and PhD (2020) in mechanical engineering from RWTH Aachen University. Since 2020, he has been with the Weichai Power European Science & Technology Innovation Center in Aachen, Germany, where he currently serves as Chief Engineer and Head of Hydraulic Component Technology. His research interests include tribology, hydraulic components (valves, pumps, motors), and hydraulic systems for off-road machinery.

Prof. Katharina Schmitz studied mechanical and chemical engineering at RWTH Aachen University and Carnegie Mellon University, Pittsburgh (USA) and graduated 2015 as Dr.-Ing. at RWTH Aachen University. Since 2018, she is full professor at RWTH Aachen University and director of the Institute for Fluid Power Drives and Systems (ifas). In addition, she is Vice Dean of the Faculty for Mechanical Engineering at RWTH Aachen, a position she holds since 2020. Prof. Schmitz's awards and honors include several best paper awards and 2023 IMechE Joseph Bramah Medal award.